Weld Heat-Affected Zones in Titanium-6Al-2Cb-1Ta-1Mo

Although good correlation between actual and simulated HAZ microstructures was obtained, it was not possible to find a cooling rate that would improve impact strength

BY J. GORDINE

ABSTRACT. The heat-affected zone in Ti-6211 was studied using Gleeble synthetic specimen techniques. Impact results from synthetic specimens indicated that poor notch ductility can be anticipated in certain regions of the heat-affected zone that are heated above 2000 F. Metallographic examination showed the structure in this region to be α^1-martensite in coarse former β grains. The cooling conditions that govern the formation of this α^1-martensite were established and attempts were made to improve the impact strength in the heat-affected zone by reducing the cooling rate. No significant improvement could be obtained and it was concluded that the poor impact properties were a result of the coarse-grained structure developed in this region.

Poor impact properties were also obtained in synthetic specimens that

were heated through weld thermal cycles having peak temperatures of 1000 to 1200 F. No change in microstructure was observed and it was concluded that this was probably a result of an ordering reaction.

Good correlation was established between actual heat-affected-zone microstructures and simulated structures produced in the Gleeble.

Introduction

Titanium-6Al-2Cb-1Ta-1Mo is one of the newer titanium alloys that have been developed to fulfill the need that exists for high strength materials for marine applications. The chief attractive property of this alloy is its insensitivity to stress-corrosion cracking which combined with its high strength to weight ratio makes it an attractive alloy for such applications.

Ti-6211 is a so-called near-alpha titanium alloy. This means that the alloy is mostly alpha with a small amount of beta. It is used in the as-forged or annealed condition because the beta stabilizing elements Cb, Ta and Mo, are not present in sufficient quantity to permit a marked increase

in strength by solution treating and aging.

The purpose of this program was to study the welding characteristics of this alloy with particular emphasis being placed on the metallurgical changes that occur in the heat-affected zone during welding.

Experimental Procedures

Material

The material used in this investigation was 0.5 in. thick Ti-6Al-2Nb-1Ta-1Mo plate supplied by Reactive Metals Inc., Niles, Ohio. The manufacturer's heat analysis is shown in Table 1.

Typical mechanical properties for the as-rolled plate material are shown in Table 2.

Metallography

Specimens for metallographic examination were carefully filed flat and then ground on silicon carbide papers down to 600 grit under running water. They were then mechanically polished with 6 micron and then 1-micron diamond and, finally, with Linde A and B. Krolls' reagent (2% HF, 6% HNO_3 in water) was used for etching.

J. GORDINE is Research Scientist, Welding Section, Physical Metallurgy Division, Mines Branch of the Department of Energy, Mines and Resources, Ottawa, Canada.

Table 2 — Typical Mechanical Properties, Plate (As-Rolled)

Thickness as-rolled, in.	Ultimate strength, psi	Tens. yield strength, 0.2% offset, psi	Compr. yield, 0.2% offset, psi	Elong. in 4D, %	Red. of area, %
1	126,000	105,000	117,000	14	30
2.5	122,000	105,000	115,000	13	28
4	120,000	100,000	113,000	12	27

Impact values — Charpy V-Notch — Ft-lb		
at +32 F	(4 in. and under)	34
at −80 F	(4 in. and under)	25

Welding Procedures

Test welds were made using the pulsed gas metal-arc (GMA) welding process. Argon trailing and underside gas shielding was used with a 75% A/25% He mixture in the torch. A 60 deg included angle double-Vee joint preparation with a 1/16 in. root face was used with a single pass being made each side. Filler metal 1/16 in. diam of the same composition as the base metal was used and welding was carried out using 20,000 joules/in. heat input (Ref. 1).

Gleeble Synthetic Specimen Techniques

Impact Testing. To evaluate the impact properties associated with individual weld heat-affected zone structures the Gleeble was used to reproduce in bulk specimens the various regions of the heat-affected zone. Charpy impact blanks, 0.400 in. square by 3.5 in. long, were machined in the rolling direction from the 1/2 in. thick plate. These blanks were then heated in the Gleeble through the various thermal cycles that are experienced in the heat-affected zone of the weld. The thermal cycles used were based on data reported by Lewis and Wu (Ref. 2) for welding 1/4 in. thick titanium plate at 25,000 joules/in. heat input (see Fig. 1). Thermal cycle peak temperatures ranging from 1000 to 2500 F in 200 F intervals were used. All treatments were made under vacuum and temperatures measured using a platinum-rhodium control thermocouple. After thermal cycling, the specimens were finish machined to standard V-notch Charpy dimensions and tolerances (Fig. 2). They were then impact tested at 32 and 70˙F.

Hot Ductility Testing. Hot ductility testing to assess the susceptibility of Ti-6211 to heat-affected-zone hot cracking during welding was carried out using the Gleeble. Specimens, 0.25 in. diam by 4 in. long, were heated at rates according to the thermal cycles shown in Fig. 1 and pulled in tension to failure at selected peak temperatures. Measurements were made of the ultimate breaking strength and the hot ductility which was measured as the percentage reduction in area.

Continuous Cooling Transformation Diagram Determination

To study the continuous cooling transformation behavior of Ti-6211, 0.25 in. diam by 4 in. long specimens were heated under vacuum to 2200 F using the Gleeble and cooled at various rates. The heating cycle used is shown in Fig. 3 together with a typical cooling curve. The cooling curve was used to determine the continuous cooling transformation diagram for the alloy. The beta to alpha transformation that occurs on cooling produces an evolution of heat that causes a discontinuity in the cooling curve as indicated in Fig. 3. By measuring the start and finish temperatures and times for the transformation, it is possible to construct a continuous cooling transformation diagram for the alloy. To standardize the time base, the point was selected at which the individual cooling curves passed through 2000 F and this was designated as time O; subsequent times were measured from this point.

Recording of the cooling curves was accomplished using the same platinum-rhodium thermocouple, already percussion welded to the Gleeble specimen, as was used for the control thermocouple on heating the specimen up to 2200 F. Different cooling rates were achieved by using gas quenching with argon or helium and for more rapid cooling rates by reducing the specimen diameter to 0.125 in.

Results and Discussion

Metallography of Ti-6211 Weldments

Test welds were made in 1/2 in. Ti-6211 plate using the pulsed GMAW process. Specimens were cross-sectioned, polished and etched, and then metallographically examined. Figure 4 shows a typical macrophotograph of such a section. The most prominent microstructural feature is the extremely coarse grained structure of the weld fusion zone. A range of structures can be observed in the heat-affected zone. Metallographic examination under higher magnification was also done and Fig. 5 shows the range of structures that are developed in the weld and in the heat-affected zone.

Figure 5A represents the structure in the fused zone at the centerline of the weld in the coarse grained region. It shows an α^1-martensite structure formed by rapid cooling from above the β-transus. Figure 5B represents another region of the fusion zone but further away from the centerline of the weld. It shows essentially the same structure with a slightly finer grain size.

Figure 5C represents a region of the heat-affected zone, immediately adjacent to the fusion zone, that has been heated during the welding process to temperatures above the β-transus where it has recrystallized and, on cooling, transformed to α^1-martensite. Figure 5D represents a region further into the heat-affected zone away from the weld centerline. It shows a recrystallized structure that has transformed, on cooling, to α^1-martensite. The original α-lath network can still be observed. Figure 5E represents a region of the heat-affected zone still further remote from the fusion zone. It shows a recrystallized structure of α^1-martensite with distinct traces of the original lath network remaining. Figure 5F shows a region of the heat-affected zone remote from the weld that has experienced temperatures below the β-transus and shows essentially the same structure as the base metal, i.e., α-laths with traces of β between them.

These results indicate that, due to the alpha to beta transformation, and the recrystallization and grain growth that occurs on heating, there is produced in the heat-affected zone a wide range of structures and due to the rapid cooling rates many of these
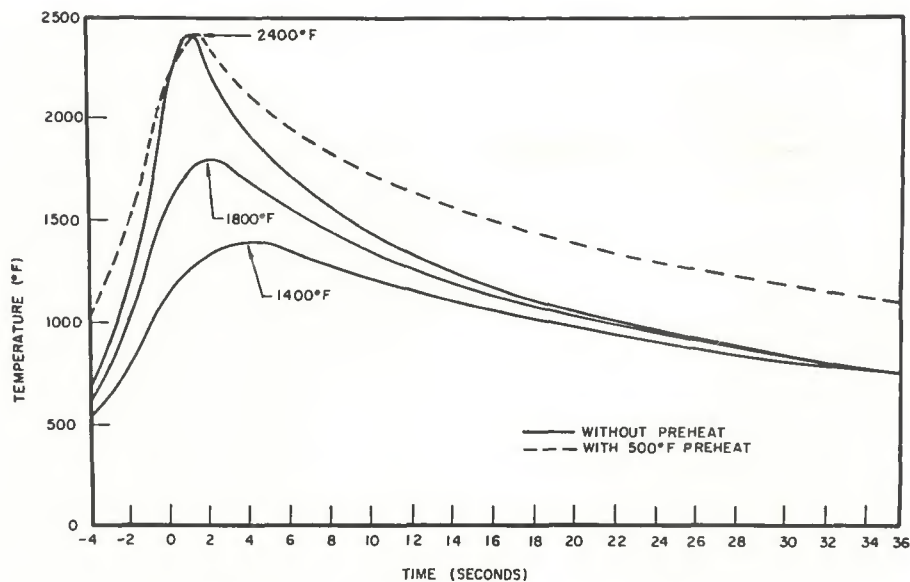
Fig. 1 — Thermal cycles in the weld heat-affected zone at three distances from the weld centerline in 1/4 in. thick titanium plate
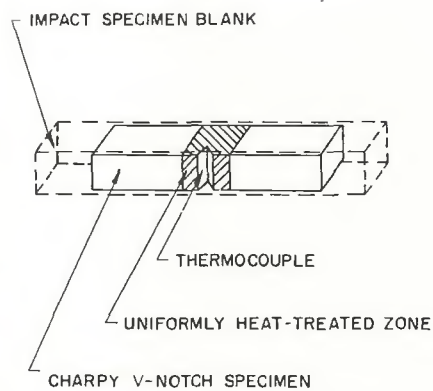

Fig. 2 — Charpy V-notch impact specimen

Fig. 3 — Typical thermal cycle used for determination of the continuous cooling transformation diagram

are non equilibrium structures. It can also be expected that associated with this wide range of structures in the heat-affected zone there will be a wide range of properties. To evaluate these properties it is necessary to use a technique whereby the various regions of the heat-affected zone can be reproduced in bulk size specimens suitable for mechanical testing. The Gleeble apparatus allows us to perform this function very conveniently.

Impact Properties of the Heat-Affected Zone

The impact properties of the heat-affected zone were evaluated using the Gleeble synthetic specimen technique. The results are shown in Fig. 6. This shows the variation in impact strength with the thermal cycle peak temperature. It is apparent that the impact properties of Ti-6211 are considerably altered by exposure to cer-
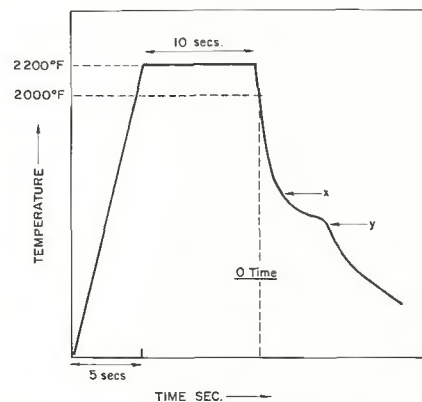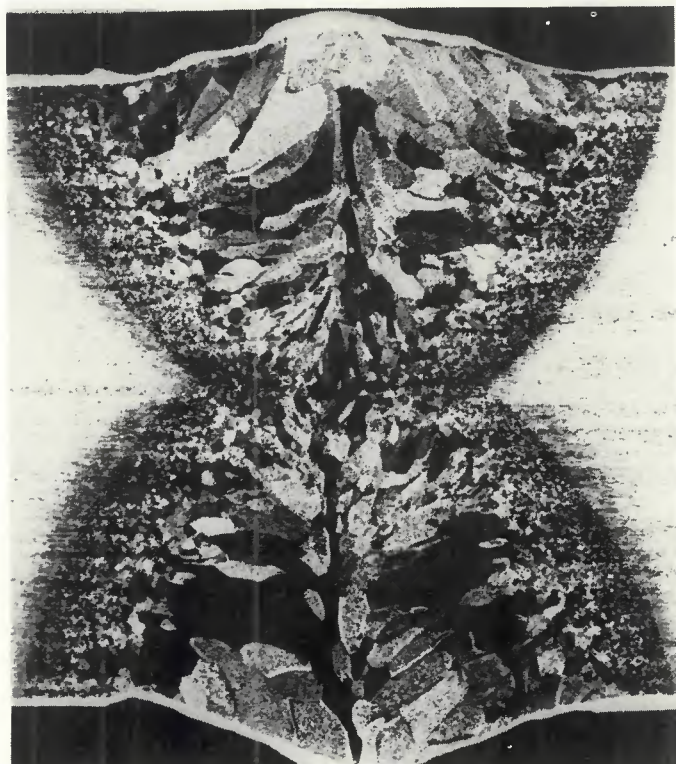

Fig. 4 — Macrograph of weldment in Ti-6211. Specimen welded by the pulsed GMAW process at 20,000 joules/in. heat input. X12, reduced 45%
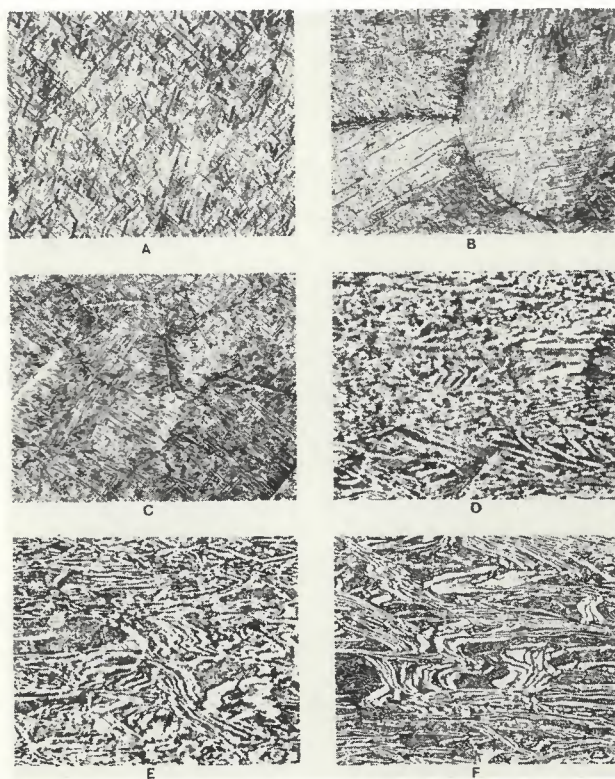

Fig. 5 — Microstructure of weld and heat-affected zone in Ti-6211. A to F represents the structures produced from the weld centerline out into the base metal. X300, reduced 50%

tain weld thermal cycles — in particular, those thermal cycles having peak temperatures above 1800 F and also thermal cycles in the range 1000-1200 F. The untreated base metal gave impact values at room temperature (70 F) and 32 F of 54 ft-lb and 49 ft-lb. Exposure to weld thermal cycles having peak temperatures of 2000 F and above reduced these impact values to between 22 and 25 ft-lb. A similar but less consistent drop was observed in specimens that underwent thermal cycles with peak temperatures in the range 1000 to 1200 F. These data indicate that the weld thermal cycles experienced in the heat-affected zone of weldments
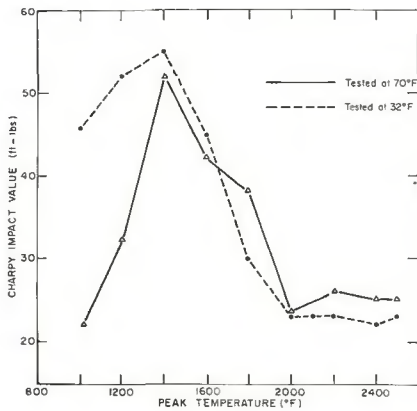

Fig. 6 — Charpy impact strength of simulated heat-affected zones of Ti-6211 as a function of thermal cycle peak temperature

of Ti-6211 will result in severe impairment of impact strength in certain regions. Some Charpy impact data on welded samples notched at the weld centerline were obtained and showed impact values of 20 ft-lb at -80 F. However, other workers (Ref. 3) report substantially higher values of 25 to 30 ft-lb at -80 F and 40 ft-lb at +32 F. It is therefore probable that certain regions of the heat-affected zone in Ti-6211 will have poorer impact strengths than the actual weld fusion zone.

Metallography of Simulated Heat-Affected-Zone Specimens

A metallographic examination of the simulated heat-affected zone impact specimens was made in an attempt to explain the impact data obtained and also to correlate the microstructures with the actual structures obtained in the heat-affected zone of the real weld.

Figure 7A shows the as-received base metal that has not undergone any thermal cycling. It shows the typical large α-laths aligned in the direction of rolling; between the laths are Widmanstatten alpha together with some small islands of retained beta. No significant changes in microstructure could be observed in specimens that had been given weld thermal cycles with peak temperatures from 1200 to 1600 F. (Fig. 7B, 7C, 7D).

However, examination of Fig. 6 shows that considerable variation in impact strength has occurred by exposure to these temperatures. This is particularly true for the room temperature impact values obtained for material that was given weld thermal cycles having peak temperatures of 1000 F and 1200 F. These specimens gave impact values of only 22 and 32 ft-lb respectively, but no changes in microstructure could be detected. One possible explanation is the ordering reaction known to occur in titanium alloys with high aluminum content on aging at 1000 F that causes embrittlement (Refs. 3, 4). Compositional variations in the alloy structure provide aluminum-rich regions (α-laths) where ordering could occur on exposure to weld thermal cycles having peak temperatures between 1000 F and 1200 F to cause this loss of impact strength.

Figure 7E shows the microstructure of the specimen that had been given a weld thermal cycle having a peak temperature of 1800 F. Here, a distinct change can be observed; the regions between the α-laths have transformed at this temperature to beta which, on cooling, transforms to α^1-martensite. This is at first surprising because the β-transus in Ti-6211 is 1860 F. However, this must be a result of the segregation of β-stabilizing alloying elements in these regions that causes a lowering of the β-transus. Consideration of Fig. 6
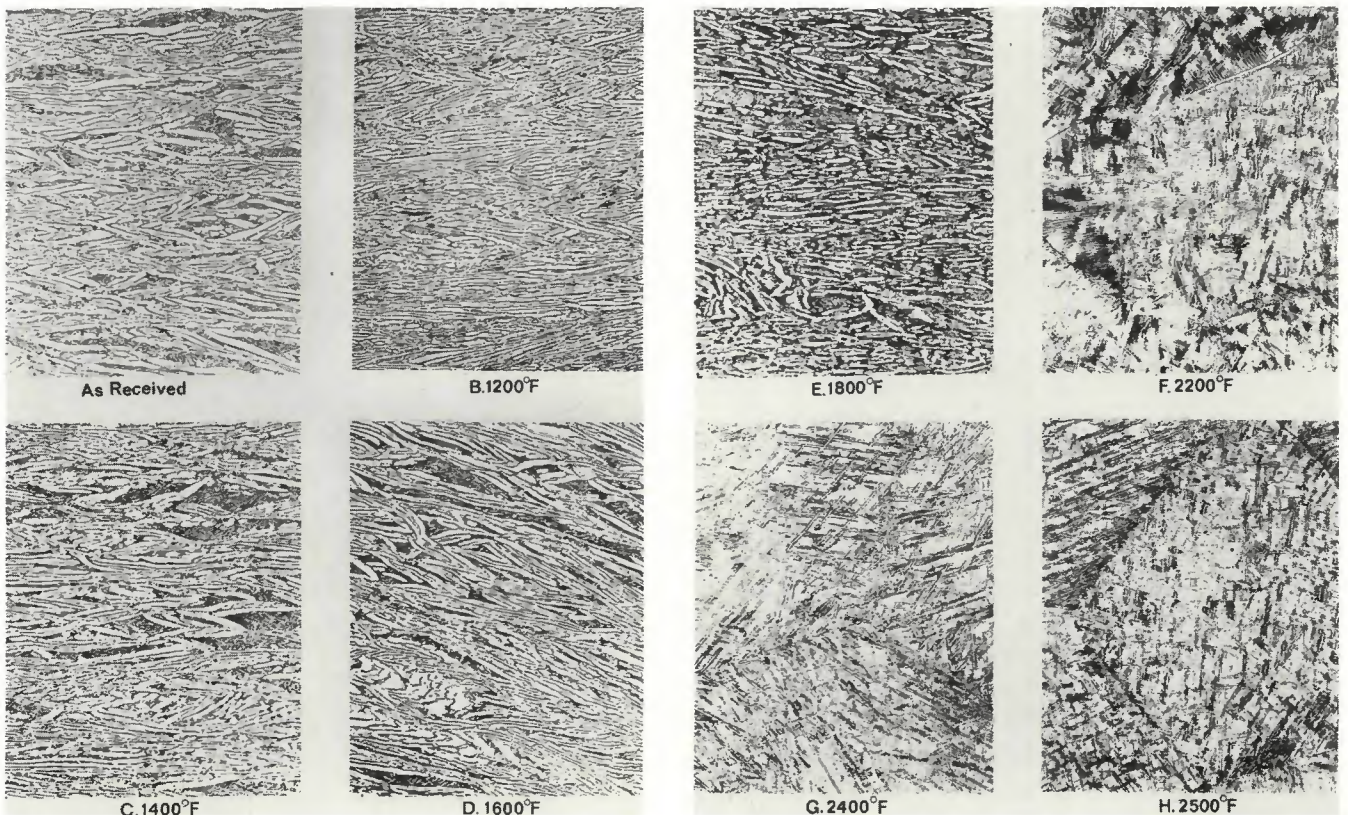
Fig. 7 — Synthetic heat-affected zone microstructure, room temperature to 2500 F. X350, reduced 45%

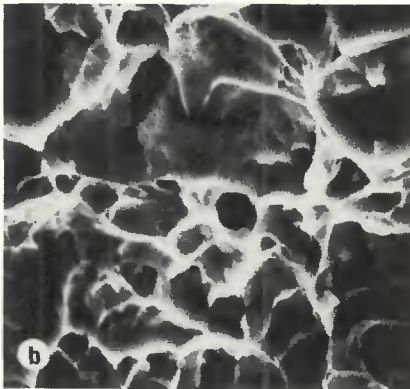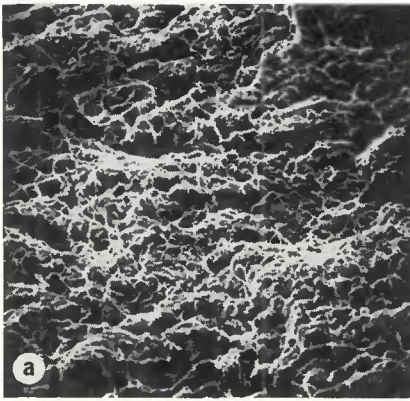Fig. 10 — Continuous cooling transformation diagram for Ti-6211

Fig. 8 — Fracture surface of impact specimen tested in the as-received condition. Scanning electron micrographs: (a) X290, (b)X1800, both reduced 47%
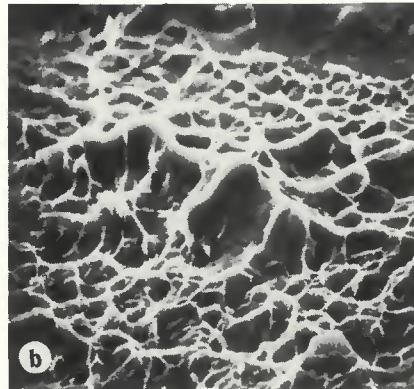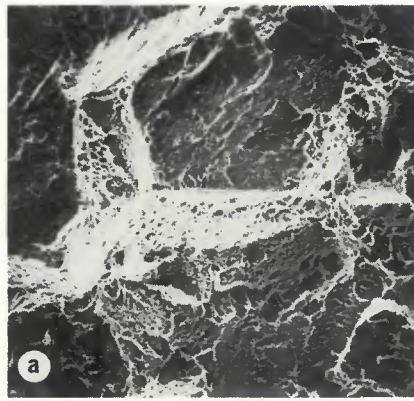

Fig. 9 — Fracture surface of impact specimen heated through a weld thermal cycle with a peak temperature 2400 F. Scanning electron micrograph: (a) X200, (b)X1960, both reduced 48%

shows that accompanying this change of microstructure is a reduction in impact strength.

Figures 7F, G and H show the microstructures of specimens that have been given weld thermal cycles having peak temperatures of 2200, 2400, and 2500 F respectively. These temperatures are above the β-transus and so complete transformation occurs to beta during the heating cycle and on cooling this will transform to equilibium alpha or to α^1-martensite. All specimens therefore show essentially the same microstructure of the criss-cross network of α^1-martensite together with some equilibrium α-platelets. Some evidence of the original α-lath network is observed in the specimens cycled to 2200 F peak temperature (Fig. 7F). At the higher peak temperatures no traces of the original structure can be observed and a mixture of α^1-platelets within coarse former β grains is produced.

Associated with this change in microstructure is a severe loss in impact properties as can be seen in Fig. 6. It would therefore appear that the poor impact properties that will be developed in those regions of the heat-affected zone that experience weld thermal cycles with peak temperatures above the β-transus (i.e., 1860 F) can be related directly to the change in microstructure. This is due to either the presence of α^1-martensite or to the very coarse grain size that is developed at these temperatures.

Examination of Charpy Fracture Surfaces of Simulated Heat-affected-zone Specimens

In addition to the metallographic examination of the Charpy specimens that had been subjected to weld thermal cycles, an examination of the fracture surfaces of some specimens was made using the scanning electron microscope. A comparison was made between the fracture surfaces of impact specimens showing low impact values that had been given weld thermal cycles with high peak temperatures (above 1800 F) and the fracture surfaces of impact specimens given no thermal cycles. Figure 8 shows the fracture surface of the specimen in the as-received condition, i.e., no weld thermal cycles. It can be observed that failure has occurred in a ductile manner; this is evi-
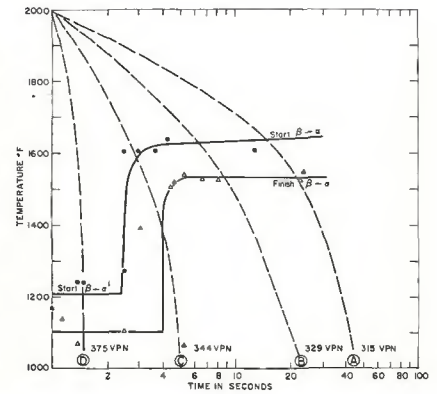
denced by the dimpled fracture surface clearly seen at higher magnification. This particular specimen gave an impact value at 32 F of 51 ft-lb.

Figure 9 shows the fracture surface of a specimen that had been subjected to a weld thermal cycle having a peak temperature of 2400 F and then broken in impact at 32 F. This particular specimen gave an impact value of only 22 ft-lb. It can be seen that failure has occurred in an intergranular manner as evidenced by the white outlines of the grain boundaries that are revealed at low magnification. Examination of the grain boundary regions at high magnification shows a dimpled fracture surface, indicating that failure has occurred in a ductile manner along the grain boundaries.

Influence of Cooling Rate on the Beta to Alpha Transformation

The impact results shown in Fig. 6 show that an embrittled zone will be developed in the weld heat-affected zone in those areas that are heated during the welding process above the β-transus and then transform to α^1-martensite on cooling. Whether this embrittlement is a result of the formation of α^1-martensite or whether it is merely a grain-size effect has not been established. It was therefore decided to investigate the cooling conditions that govern the formation of α^1-martensite rather than the equilibrium alpha predicted by the equilibrium diagram and to then relate this data to the mechanical properties that will be developed in the heat-affected zone.

To do this, a continuous cooling transformation diagram was determined, using the thermal arrest technique, that could be used to predict the structures that will be developed when cooling from temperatures at which the structure is entirely beta. This is particularly useful for consideration of the structures that can be anticipated in a weldment, because in

Rate A   315 VPN

Rate B   329 VPN

Rate C   344 VPN

Rate D   375 VPN

Fig. 11 — Typical microstructures of specimens used to determine continuous cooling transformation diagram. Cooling rates correspond to the cooling curves shown in Fig. 10. X400, reduced 25%

Fig. 12 — Influence of cooling rate from 2400 F on the microstructure produced. (a) argon quench, (b) cooled 5 F/sec, (c) isothermal 1700 F. X500, reduced 32%

this case, all of the weld and at least part of the heat-affected zone must cool very rapidly from the beta region.

Figure 10 shows the continuous cooling transformation diagram that was developed. Similar data have been reported by Mitchell and Tucker (Ref. 6) in a titanium-6Al-2Sn-4Zr-2Mo alloy using the same thermal arrest technique. This diagram describes how beta will transform to either α or α^1-martensite, depending upon the cooling rate.

Superimposed on the diagram are four typical cooling rates together with hardness values obtained for the specimens cooled at these various rates. One immediate observation from these results is that the hardness is a function of the rate of cooling. Rapid cooling (Rate D) gave an approximately 60 point increase in hardness over specimens cooled at slower rates (Rate A). It is also very apparent that the rate of cooling has

a marked influence upon the temperature at which the transformation of beta to alpha or α^1 occurs. Very rapid cooling rates can suppress these transformation temperatures to quite low temperatures ($\sim$1200 F).

The microstructures produced in specimens cooled at the four different cooling rates indicated in Fig. 10 are shown in Fig. 11. Slow cooling rates such as cooling rate A produced a soft α-platelet structure as shown in Fig. 11A. As the cooling rate was increased, a finer α-platelet structure together with increased hardness was obtained, as can be seen in Figs. 11B and 11C. At the most rapid cooling rates, such as cooling rate D, that miss the knee of the continuous cooling transformation diagram, a fine criss-cross needle-like α^1-martensite is produced as can be observed in Fig. 11D. No α-platelets can be seen in the structure and this structure has the highest hardness, 375 VPN.
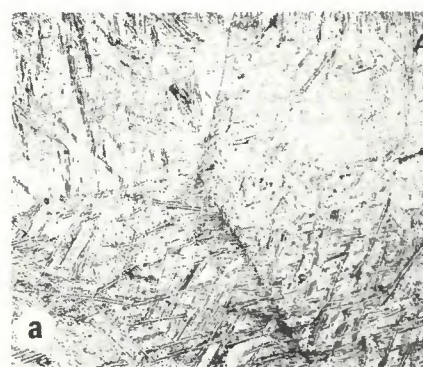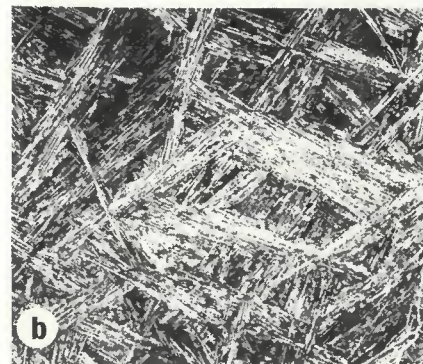
These results show that depending upon the cooling rate beta can transform to α^1-martensite or to equilibrium alpha. Examination of microstructures developed in the weldments of Ti-6211 and in regions of the heat-affected zone that were heated during welding to temperatures above the β-transus showed structures of essentially α^1-martensite with traces of equilibrium α-platelets. (Fig. 5A, B, C and D) As these microstructures also showed poor impact properties (Fig. 6 and 7E, F, G, H) it was decided to see what effect varying the rate of cooling would have on the impact properties.

Influence of Cooling Rate on the Impact Properties

The effect of varying the rate of cooling from temperatures above the β-transus was studied. A series of impact specimens were heated in the
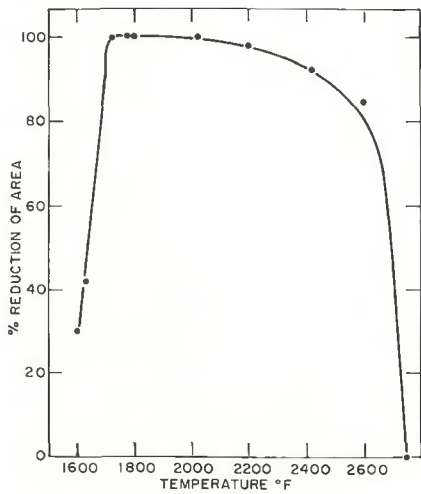
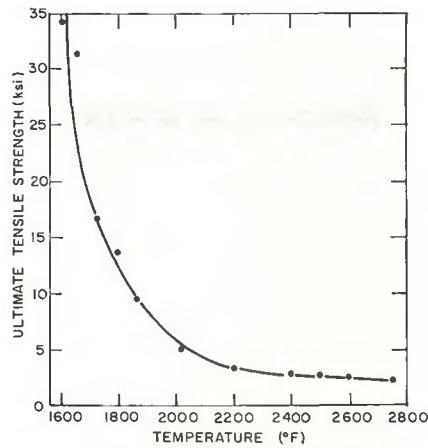Fig. 13 — Percentage reduction of area as a function of test temperature

Fig. 14 — Ultimate break strength as a function of test temperature

1605°F   1780°F   1860°F
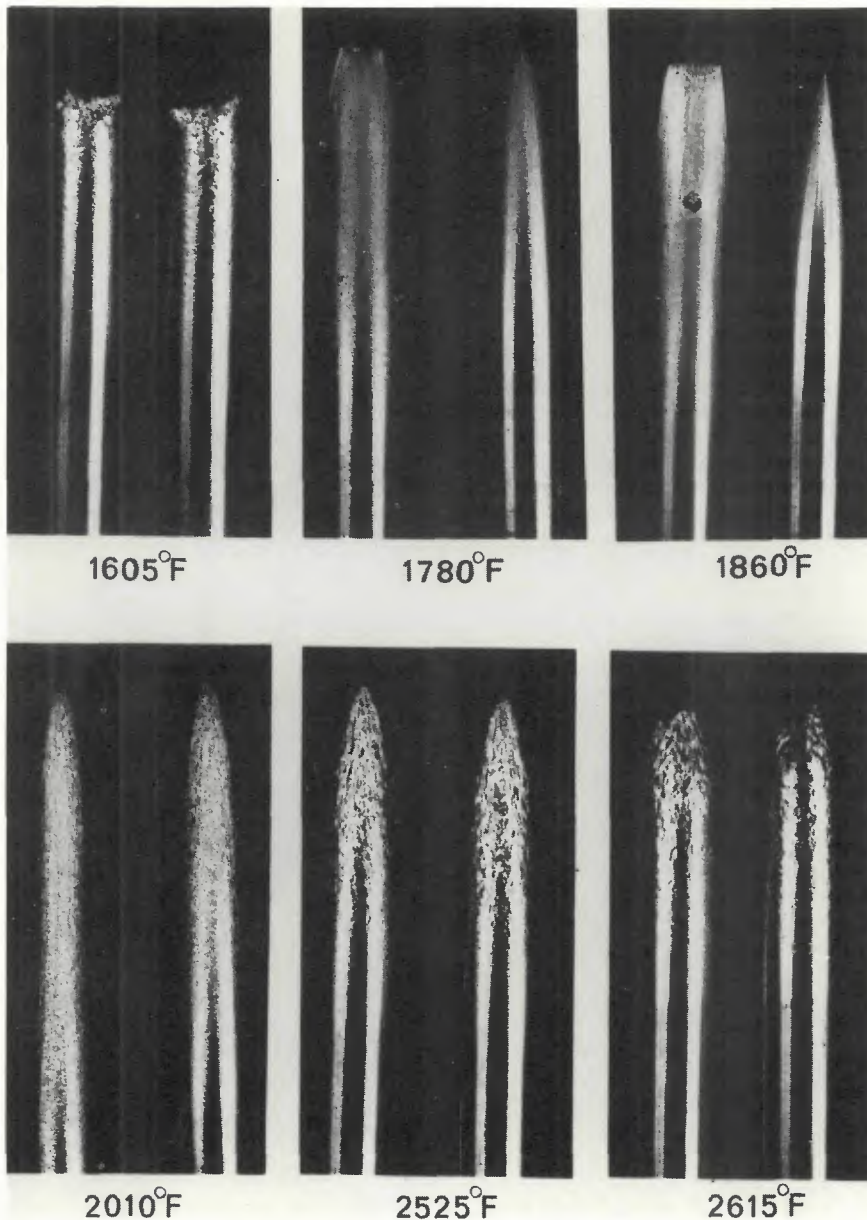
2010°F   2525°F   2615°F

Fig. 15 — Typical fracture appearances of hot ductility specimens

Gleeble to 2400 F according to the thermal cycle shown in Fig. 1 and cooled from this temperature at different rates. The variation in cooling rate was achieved by gas cooling and by programmed cooling. The specimens were then impact tested at 32 F. Table 3 shows the results.

These results indicate that the impact strength of simulated heat-affected zone specimens is relatively insensitive to the rate of cooling. Rapid cooling rates such as are provided by helium and argon gas quenching gave slightly better values of impact strength than did specimens that were cooled at slow programmed rates. Isothermal transformation at 1700 F gave some improvement in impact strength but the effect was not of great significance.

Metallographic examination of the specimens cooled at different rates was carried out. Figure 12A shows the microstructure produced by gas quenching in argon from 2400 F. This cooling rate misses the "knee" of the continuous cooling transformation diagram (Fig. 10) and hence produces the characteristic α^1-martensite structure. Figure 12B shows the microstructure produced by slow cooling at 5 F/sec from 2400 F, and reveals an α-platelet structure. Despite these differences in microstructure, both cooling conditions gave approximately the same impact strengths. Figure 12C shows the microstructure produced by cooling from 2400 to 1700 F and isothermally transforming at this temperature for ½ h and then cooling to room temperature. The structure obtained is of very coarse α-platelets. This can be predicted from the continuous cooling transformation diagram (Fig. 10). Holding at 1700 F will allow the beta to transform in an equilibrium manner to alpha. However, this equilibrium alpha structure does not possess significantly better impact properties than the rapidly cooled α^1 structures.

It can be concluded that the low impact strength in the β-heated structures is associated with intergranular fracture and is insensitive to cooling rate and the presence of α^1 or equilibrium alpha. It is therefore a β-grain size effect. Thus no real improvement can be achieved by reducing the cooling rate in the heat-affected zone.

Hot Ductility Testing

Hot ductility tests were made using the Gleeble to assess the susceptibility of Ti-6211 to heat-affected zone hot cracking during welding. It was not possible to complete this part of the work owing to difficulties encountered with alloying of the control thermocouple with the titanium alloy

Table 3 — Impact Strength Values for Various Cooling Rates

Cooling rate from 2400 F	Impact strength at 32 F, ft-lb
Helium gas quench	20
Argon gas quench	22
Programmed cooling at 20 F/sec	19
Programmed cooling at 5 F/sec	18
Thermally transformed for ½ h at 1700 F	24

that caused detachment of the thermocouple on exposure to high peak temperatures above 2000 F. Sufficient data were developed, however, to produce the so-called "on-heating" curve, and this is shown in Fig. 13. Development of the "on-cooling" curve, i.e., heating through the weld thermal cycle to the zero-ductility temperature, in this case 2750 F, and testing on cooling from this temperature, was not possible due to detachment of the control thermocouple at these temperatures.

The "on-heating" curve of Fig. 13 shows a quite normal behavior; the ductility as measured by percentage reduction in area rises to a maximum in the range 1700 to 2000 F and falls off gradually with a sudden drop above 2600 F to zero ductility. This type of behavior is typical of a material not susceptible to heat-affected zone hot cracking. The ultimate tensile strength as a function of test temperature is shown in Fig. 14. This again exhibits quite normal behavior, the ultimate tensile strength falls off quite rapidly over the range 1600 to 2000 F and then settles to a constant low level.

The rather low ductility values obtained at 1600 F are probably not of great significance, because at this temperature the strength level is still quite high. There is a change in fracture mode above about 1900 F due to the change in structure from the close-packed hexagonal alpha to body-centered cubic beta that occurs at 1860 F. (see Fig. 15) This apparently has little influence, however, on the ductility values and strength values obtained.

Conclusions

Welding procedures for Ti-6211 were established using the pulsed GMAW process and sound quality welds were produced. Hot ductility tests made with the Gleeble did not show any anomalous behavior and did not indicate a susceptibility to hot cracking.

Detailed examination of the heat-affected zone using synthetic specimen techniques revealed that some problems may be anticipated. Poor impact strengths, lower than those of the weld fusion zone are developed in the areas of the heat-affected zone immediately adjacent to the fusion zone; specifically those regions which reach temperatures above 1800 F. The structure developed in these regions in equilibrium α-platelets with α^1 martensite within coarse former beta grains produced as a result of rapid cooling from a temperature at which it is fully beta.

Attempts to improve the impact values by changing the cooling conditions were not successful. Slowing down the cooling rate by using for example, preheating, will replace the α^1 with equilibrium α-platelets but does not improve the notch ductility in the heat-affected zone. Isothermal transformation at 1700 F did give some improvement but is of little practical significance. It is considered that the poor impact strengths of these regions are mainly a result of the coarse grain size.

Welding should therefore be done using low heat inputs in order to minimize the width of the heat-affected zone. Reduced impact strengths in regions of the heat-affected zone that reached temperatures of 1000 to 1200 F are thought to be due to an ordering reaction. Good correlation was established between actual heat-affected zone microstructures and simulated structures produced in the Gleeble.

References
1. Nolan, M. J., P.M.D. Progress Memorandum Feb. 1970.
2. Lewis, R. E. and Wu, K. C., "A Study of the Weld Heat-Affected Zone in the Titanium-6Al-6V-2Sn Alloy." *Welding Journal*, Vol. 42 (6), June 1963, Res. Suppl., 241-s.
3. Stark, L. E., "Welding Evaluation of Ti-6Al-2Cb-1Ta-0.8Mo Alloy Plate." Research Report R 481, December 1966, Reactive Metals, Niles, Ohio.
4. Clark, D., Jepson, K. S., Lewis, G. I., "A Study of the Ti-Al System up to 40 Atomic % Al." *J. Inst. Metals*, 1962, 91, 197.
5. Saltis, P. J., "Instability and Evidence of Ordering in Ti-8Al-1Mo-1V Alloys." *Trans. AIME 1965*, 233, 903.
6. Mitchell, D. R. and Tucker, T. J., "The Properties and Transformation Characteristics of Welds in Ti-6Al-2Sn-4Zr-2Mo Titanium Alloy," *Welding Journal*, Vol. 48 (1), January 1969, Res. Suppl., 23-s.

WELDING METALLURGY | *Concisely presented information of great value to everyone in the industry*

WELDING METALLURGY, by George E. Linnert, offers a concise but comprehensive treatment of the great mass of technical information now available in this field. The subject matter is divided into two volumes.

Volume I — Fundamentals — is designed to provide the basic information necessary for any real understanding of welding as a major tool of the steel fabricating industry. It begins with the essentials of welding and metallurgy, considered separately. It concludes with a study showing how the welding thermal cycle alters the microstructure of the joint and how this alteration, in turn, affects joint properties.

In Volume II — Technology — the earlier material is developed in greater detail, focusing on the specific factors and conditions that require consideration when dealing with particular projects. The discussions, illustrations, and data tables in Volume 2 again follow the basic metallurgical approach to each subject area. In this manner, a strong understanding of the basics is provided, which the reader may easily reinforce by specialized study into whatever other aspects are deemed important.

These two volumes will prove useful not only in orienting the novice welding engineer to this broad field of welding, but also in helping the more experienced professional who needs assistance in finding a rational basis for solving problems.

Volume I, Fundamentals $12.00
Volume II, Technology $14.00

Discounts: 25% to A and B members; 20% to bookstores, public libraries and schools; 15% to C and D members.

Send your order to the American Welding Society, 2501 NW 7th St., Miami, FL 33125. Florida residents add 4% sales tax.

WELDING INSPECTION | *An introduction to the subject that even experienced inspectors will refer to often*

WELDING INSPECTION describes the general duties and responsibilities of inspectors of weldments. Because the discussions are more general than those found in particular codes and specifications, it is especially useful for training inspectors.

Among the topics covered are: requirements for an inspector; duties of an inspector; welding procedure specification; qualification of welding procedures; qualification of welders and welding operators; weldment defects, and destructive and nondestructive testing of welds. $9.00.

Discounts: 25% to A and B members; 20% to bookstores, public libraries and schools; 15% to C and D members.

Send your order to the American Welding Society, 2501 NW 7th St., Miami, FL 33125. Florida residents add 4% sales tax.